Zirconium aluminides studied with first principles calculations: hyperfine interactions and site preference of dopants

A. Kapidžić, J. Belošević-Čavor*, V. Koteski

Vinča Institute of Nuclear Sciences, National Institute of the Republic of Serbia, University of Belgrade, Belgrade, Serbia

Abstract

By means of a density functional theory (DFT) based augmented plane waves plus local orbitals (APW + lo) method, we study the electric field gradients (EFG) in Ta and Cd-doped Zr-Al intermetallics. Comparing the obtained results with the experimental data obtained from the perturbed angular correlation (PAC) measurements, we conclude that Ta atoms always replace Zr in all the investigated compounds. Our results confirmed the previous experimental assumption that Cd substitutes exclusively for Al in $ZrAl_3$ and Zr_2Al_3. In the case of Zr_2Al our calculations suggest that Cd can probably substitute on both Zr and Al lattice sites, while in Zr_3Al, it is most likely to occupy Al position. The effects of the distance between the impurity atoms in the supercells and the deviation of the c/a ratio are also discussed.

Keywords: first principles calculations; hyperfine interactions; zirconium aluminides; impurity atoms

1. Introduction

The Zr-Al phase diagram is rather complicated, as it exhibits ten intermetallic compounds with narrow concentration ranges and different crystal structures (hexagonal, orthorhombic, tetragonal, and cubic) [1, 2]. Zirconium-aluminum intermetallics are of prime interest for high-temperature structural usage, due to their superior physical and chemical properties, such as corrosion

*Corresponding author: e-mail cjeca@vinca.rs, fax +381-11-3408-681, phone +381-11-3408-549

resistance, low absorption cross-section for thermal neutrons, low thermal expansion coefficients, outstanding biocompatibility, and light weight in combination with relatively high strength [3]. Consequently, numerous studies have been conducted to investigate their structural [4, 5], mechanical [6], thermodynamic [7, 8], and superconducting [9] properties. Besides extensive work has been reported regarding the amorphization [10-17], oxidation [18-20], phase formation [21, 22], high pressure torsion [23], and Fermi surface properties [24] of Zr-Al alloys. Ab initio methods based upon density functional theory have also been employed to derive a number of their properties including lattice parameters, elastic constants, the relative stability of competing structures, heats of formation, and point defects [25-36].

The present work aims to reveal the site preference of added impurities, in particular Ta and Cd, in Zr-Al intermetallics, through the calculation of hyperfine interaction parameters (electric field gradients and asymmetry parameters), which is important for understanding and controlling their physical, mechanical and chemical properties. Namely, the properties of metals, intermetallic phases and superalloys can be tailored by doping with suitable alloying elements and the site preference of dopant atoms can have significant impact on their properties. For example, introducing refractory elements in Ni [37] and Ni-base superalloys [38] improves their mechanical properties and corrosion resistance. In that sense it is important to gain insight into the local structure and possible lattice relaxation around dopant atoms.

The electric field gradient (EFG) depends on the nearest neighbor charge distribution and as such is particularly sensitive to the asymmetry of the charge density in the vicinity of the impurity atom. Because of its local sensitivity, it is an optimal tool to study local atomic structure around the impurity atom and to determine the impurities localization. It can be measured by perturbed angular correlation (PAC) technique in which each position of the probe (impurity) atom usually

gives its own characteristic and distinguishable signal. However, this information is rather indirect and the interpretation of the measured results often requires highly accurate ab initio calculations. So far, a systematic PAC study of the hyperfine interaction parameters with Ta and Cd probes in the full series of zirconium aluminides has been conducted [39-44] and for some compounds ($ZrAl_2$, Zr_3Al_2, Zr_4Al_3) successful attempts have been made to assign them to the possible Zr and Al lattice sites [45-47]. As it has been shown, Ta probes usually occupy Zr lattice sites, due to the strong chemical similarity of the Ta radioactive mother isotope (^{181}Hf) to zirconium, but the situation with ^{111}In/^{111}Cd probe is much more complicated, due to the competition between atomic size and electronegativity criterion. In this respect the goal of the present work is to assign the measured EFGs to the possible crystal structures and crystallographic sites in different Zr-Al intermetallic compounds (ZrAl, Zr_2Al, Zr_3Al, $ZrAl_3$, and Zr_2Al_3).

2. Calculation details

The calculations were done using the density functional theory based augmented plane wave plus local orbital (APW + lo) method within the WIEN2k code [48]. Exchange and correlation effects were treated using the general gradient approximation by Perdew, Burke and Ernzerhof (PBE) [49]. The atomic spheres radii of 2.3 a.u. for Al, 2.6 a.u. for Ta and 2.5 a.u. for Zr and Cd were used. The $R_{MT}k_{max}$ parameter for limiting the size of the basis set, was set to 8.0 for pure (undoped) systems and to 7.0 for the doped ones. The Brillouin zone integrations were performed via a tetrahedron method [50] with 168-865 k points in the irreducible wedge of the Brillouin zone for the undoped systems and 48-84 k points for the doped ones, depending on the size of the (super)cells. The core states were treated fully relativistically, while the valence states were treated within the scalar relativistic approximation. The self-consistency of the calculations was provided through the charge convergence criterion, demanding that the integrated charge difference to be

smaller than 5 x 10^{-5} electrons. After determing the self-consistent charge density and potential, the electric field gradient tensor V_{ij} was calculated using the method from the Ref. [51], with the largest component designated by the convention as V_{zz}. The asymmetry parameter η is defined as $(V_{yy}-V_{xx}) / V_{zz}$, where $|V_{zz}| > |V_{yy}| > |V_{xx}|$.

Structural relaxation was done in regard to the internal structure parameters and lattice constants. First the atomic positions were relaxed in accordance with the calculated Hellmann-Feynman forces until the force on each atom was smaller than 2 mRy/a.u. and then theoretical equilibrium volumes and if necessary, depending on the crystal structure, c/a and b/a ratios were determined. The lattice constants obtained in this way were used for the construction of the supercells, whose sizes were chosen depending on the size of the original cell (2 x 2 x 2 for Zr_2Al and Zr_3Al, 3 x 1 x 2 for ZrAl, 4 x 4 x 1 for $ZrAl_3$ and 1 x 1 x 2 for Zr_2Al_3). Finally, a single host atom, either Zr or Al, was replaced by one of the probe atoms that are used in PAC measurements (Ta and Cd), in order to compare our calculated V_{zz} and η values with the measured ones and in that manner determine the site preference of the probe atoms. Such constructed supercells are presented in Figures 1 and 2 using XCrysDen program [52].

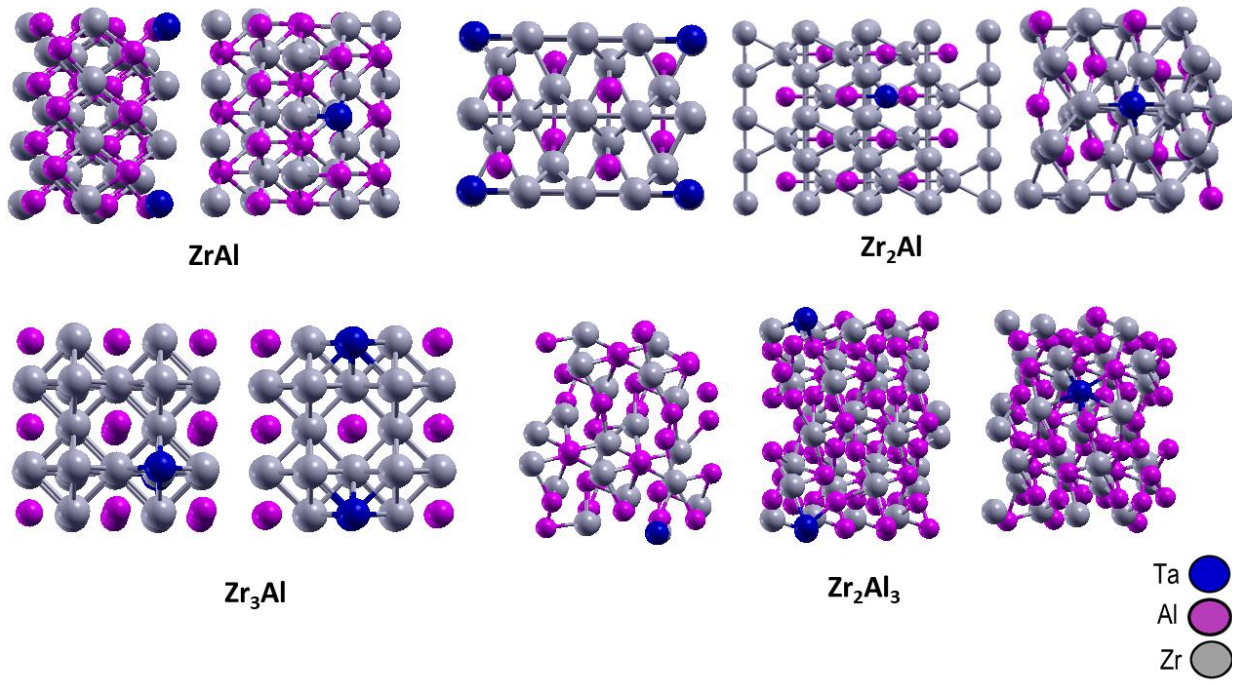

Figure 1: Models of the supercells used in study for four Zr-Al compounds

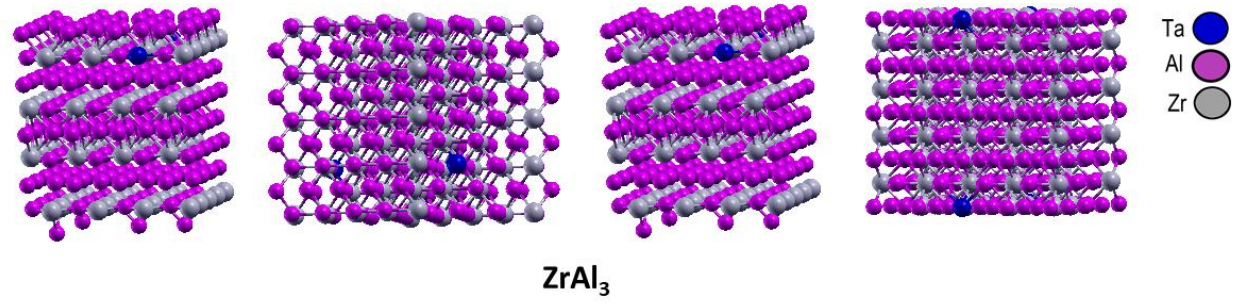

Figure 2: Models of four types of supercells for $ZrAl_3$ used in calculations

3. Results and discussion

3.1. Structural parameters

The calculated internal parameters and lattice constants for the investigated compounds, along with the experimental values obtained from X-ray diffraction measurements [7, 24, 53, 54] and the earlier calculations [25, 26, 27, 29, 31, 33, 34, 35] are given in Table 1. In all cases the theoretically determined volume overestimates the experimental one, which is expected due to the well-known fact that DFT calculations with a common GGA exchange-correlation functional systematically overestimate the ground-state volume [55]. However, in our calculations the overestimation is not large and it ranges from 0.5% for Zr_3Al to 0.8% for $ZrAl_3$ and Zr_2Al_3. When it comes to c/a ratio, the calculated values are close to the measured ones and differ no more than 0.2%, except in the case of ZrAl, where this difference reaches 1.5%. As for the b/a ratio, in Zr_2Al_3 it is almost the same as the measured one (differs by 0.09%), while in ZrAl the deviation is somewhat larger (0.8%). The bulk moduli B_0, obtained by fitting the data to the Murnaghan's equation of state [56] are also given in Table 1. To the best of our knowledge, there is no experimental information regarding the bulk moduli in these compounds, but when compared to the earlier calculations, our values exhibit good agreement.

Table 1: The parameters of the investigated structures

Structure parameters	WIEN2k	Earlier calculations [25, 26, 27, 29, 31, 33, 34, 35]	Experimental results [7, 24, 53, 54]
ZrAl (space group Cmcm)			
a [Å]	3.396	3.360, 3.3603	3. 362, 3.353
b [Å]	10.924	10.961, 10.877	10.903, 10.892
c [Å]	4.257	4.288, 4.2696	4.281, 4.274
B [GPa]	108.4	106.81	
Zr 4c	0 0.160 0.25	0 0.1612 0.25, 0 0.15947 0.25	0 0.166 0.25
Al 4c	0 0.4285 0.25	0 0.42874 0.25, 0 0.42842 0.25	0 0.424 0.25
Zr_2Al (space group $P6_3/mmc$)			
a [Å]	4.907	4.908, 4.923, 4.862, 4.8882	4.894
c [Å]	5.936	5.929, 5.928, 5.940, 5.860, 5.8798	5.928
B [GPa]	103.8	102.16, 103.1, 102.76, 100.6, 110.1	
Zr_3Al (space group Pm-3m)			
a [Å]	4.381	4.380, 4.375	4.372
B [GPa]	100.1	102.028, 98.706	
$ZrAl_3$ (space group I4/mmm)			
a [Å]	4.018	4.020, 4.0082	3.9993, 4.007
c [Å]	17.323	17.329, 17.2969	17.283, 17.286
B [GPa]	103.1	102.07	
Zr 4e	0 0 0.1188	0 0 0.1182, 0 0 0.11851	0 0 0.1191
Al 4e	0 0 0.3751	0 0 0.37442, 0 0 0.37502	0 0 0.3751
Zr_2Al_3 (space group Fdd2)			
a [Å]	9.625	9.648, 9.6949	9.601
b [Å]	13.953	13.936, 13.8994	13.906
c [Å]	5.574	5.599, 5.5705	5.574
B [GPa]	108.3	106.52	
Zr 16b	0.1826 0.0527 0.0049	0.18277 0.05276 0, 0.18270 0.05266 0.00234	0.185 0.052 0
Al 8a	0 0 0.6195	0 0 0.59987, 0 0 0.61831	0 0 0.62
Al 16b	0.1818 0.1350 0.4964	0.18170 0.11485 0.5, 0.18170 0.13514 0.49351	0.18 0.125 0.5

3.2. Hyperfine interactions

In order to compare our calculated results for the largest component of the diagonalized EFG tensor, V_{zz} and asymmetry parameter η, with the corresponding measured values obtained from PAC experiments and thus determine the site preference of the dopants, we constructed supercells

in which a Zr or Al atom was substituted by a Cd or Ta probe atom. The point group symmetry around the impurity atom remained the same as around the original atom, but the substitution led to the increase of the number of nonequivalent atoms in the cells and produced non-negligible forces on the neighboring atoms. All atoms in the supercells were allowed to relax to new equilibrium position until the forces on them were below 2 mRy/a.u. The hyperfine interaction parameters, V_{zz} and η, of Ta and Cd located at all possible crystallographic sites in all the investigated phases were calculated and the results are presented in Table 2. Because the ab initio calculations provide values at T = 0K, the extrapolation of the measured V_{zz} to zero temperature are also given in Table 2. We also predict the signs of the V_{zz}, which have not been determined from the experiments.

We first note that the calculations reproduce the measured hyperfine interaction parameters in $ZrAl_3$ and Zr_2Al_3 very well, but in the ZrAl, Zr_2Al and Zr_3Al the differences between the calculated and measured values are larger, especially for the Cd impurity atom. As expected, Ta probe atoms always occupy Zr sites in all the investigated compounds and the calculated V_{zz} values for this probe differ from the measured ones for about 10%, which is in accordance with the estimated errors for the EFG calculated within the DFT with standard exchange-correlation functionals [57]. The only exception is minority EFG component in Zr_2Al with frequency of 43 MHz, which was tentatively assigned to the Zr 2d site [39], but according to our calculations it actually belongs to the Zr 2a site. In this case we found a serious discrepancy in V_{zz}, by a factor of 2, which is probably a consequence of the small V_{zz} value at this site. Besides, in this case it is difficult to compare the calculated V_{zz} value with the measured one at 0K, as its temperature behavior is unusual and irregular, so the extrapolation of the measurement to 0K is hardly possible.

Table 2: Comparison between the calculated and measured EFG values

Compound	Probe	Lattice site	Vzz [10^{21} V/m^2] calculated	η calcu-lated	Vzz [10^{21} V/m^2] measured [39-42]	η measu-red	Vzz [10^{21} V/m^2] extrapolated to 0K
ZrAl	^{181}Ta	Zr 4c	-18.3	0.39	18.7	0.46	19.7
		Al 4c	19.9	0.21			
	^{111}Cd	Zr 4c	-6.9	0.12	~5.0 (5.5)		
		Al 4c	8.7	0.36			
Zr_2Al	^{181}Ta	Zr 2a	1.4	0	0.7	0	irregular, ~0.9
		Zr 2d	17.9	0	19.4	0	20.0
		Al 2c	-13.9	0	-	-	
	^{111}Cd	Zr 2a	-2.4	0	-	-	
		Zr 2d	5.1	0	6.8	0	7.4 (8.1)
		Al 2c	1.0	0	-	-	
Zr_3Al	^{181}Ta	Zr 3c	-9.8	0	11.0	0	11.7
		Al 1a	0	0	-	-	
	^{111}Cd	Zr 3c	-11.2	0	1.4	0	1.28
		Al 1a	0	0	0	0	
$ZrAl_3$	^{181}Ta	Zr 4e	-4.8	0	4.85	0	4.89
		Al 4e	14.6	0	-	-	
		Al 4d	-13.3	0	-	-	
		Al 4c	12.0	0.28	-	-	
	^{111}Cd	Zr 4e	-2.6	0	-	-	
		Al 4e	8.5	0	-	-	
		Al 4d	-5.1	0	4.31	0	4.45 (4.85)
		Al 4c	9.3	0.06	-	-	
Zr_2Al_3	^{181}Ta	Zr 16b	-6.8	0.68	6.87	0.4	7.20
		Al 8a	-16.3	0.04			
		Al 16b	-17.3	0.73			
	^{111}Cd	Zr 16b	-3.0	0.59			
		Al 8a	6.8	0.64	5.82	0.51	6.04 (6.58)
		Al16b	8.9	0.46	7.57	0.47	7.88 (8.59)

When it comes to Cd probe atoms the situation is much more complicated. In particular ^{111}In / ^{111}Cd PAC spectrum, taken at room temperature (RT) for the $ZrAl_3$ sample [42] is characterized by a single EFG of ≈ 4.3 x 10^{21} V/m^2 (4.5 x 10^{21} V/m^2 after the extrapolation to 0K), which can obviously be assigned to the case of Cd substituting Al 4d position in $ZrAl_3$. The measured PAC spectrum for ^{111}Cd probes in Zr_2Al_3 [42] showed two asymmetric EFGs of 7.57 x 10^{21} V/m^2 and

5.82 x 10^{21} V/m^2 at RT, which were tentatively assigned on the basis of the fraction's ratio to the Cd at the Al 16b and Al 8s lattice sites, respectively. Our calculations confirmed this assignment undoubtedly. The PAC spectrum of Zr_2Al at RT [39] exhibits two EFGs with asymmetry parameters equal to zero. Most of the probes experience EFG of 6.8 x 10^{21} V/m^2, which according to our calculations can originate only from Cd placed at Zr 2d site in Zr_2Al, although the calculated EFG deviates from the experimental value by 30%. The second EFG of 1.4 x 10^{21} V/m^2, was assigned to Cd probe on Zr lattice site in the Zr_3Al, due to occurrence of the similar component in Zr_3Al and the existence of a small admixture of the Zr_3Al phase in the Zr_2Al sample [39]. However, our calculations indicate that this component could also stem from Cd substituting Al 2c or even Zr 2a atoms in Zr_2Al, especially taking into account the absence of the frequency characteristic for the Zr_3Al phase in the same Zr_2Al sample measured with ^{181}Ta probe [39]. In fact, our calculated V_{zz} value for Zr 3c in Cd doped Zr_3Al is ten times larger than the V_{zz} which corresponds to this frequency, so we can exclude the possibility that it belongs to the situation when Cd substitutes Zr atoms in Zr_3Al, although we cannot give explanation for its origin.

As for the ZrAl, the PAC spectra taken with ^{111}In/^{111}Cd probes in this sample, showed that about 50% of probes were located in the Zr_2Al_3 contaminating phase and the rest of the probes experience a broad EFG distribution of about 5 x 10^{21} V/m^2 [40]. We can only speculate that this EFG could originate from Cd at Zr site in ZrAl, as there is no information about its temperature dependence and asymmetry parameter, so it is difficult to make a comparison.

In conclusion, Ta probe atoms always prefer Zr positions, while Cd can settle on both Zr and Al position in the crystal lattice. Because of the nature of the PAC method, in which the measured samples are doped with radioactive probes which decay, we have to consider the radioactive parent of ^{111}Cd and ^{181}Ta, namely ^{111}In and ^{181}Hf, respectively, in order to explain the preferential site

occupation. Generally, site preference of dopants depends on their atomic volume and electronegativity. As can be seen from figure 3, Hf (Ta) atoms are expected to incorporate on the Zr site, because of their similar atomic volumes and electronegativities. However, the data on In (Cd) probe position is more difficult to explain. On the one hand In and Al are located in the same group of periodic table and there is a small difference in their electronegativities, which should favor substitution of Al by In, but on the other, there is a large difference in their atomic volumes and atomic radii. Analyzing interatomic distances in the investigated structures we come to the conclusion that, when Cd replaces Zr or Al, in the compounds where the distance between In (Cd) probe atom and nearest neighbor atoms is similar ($ZrAl_3$, Zr_2Al_3), closeness in electronegativities prevails and In (Cd) substitutes Al atoms. In the case where settling In (Cd) atom on Al site produces structure with significantly smaller interatomic distance between Cd probe atom and nearest neighbors than in the case when it would be on Zr site (ZrAl, Zr_2Al), the factor of atomic volume prevails and Cd settles on Zr lattice position.

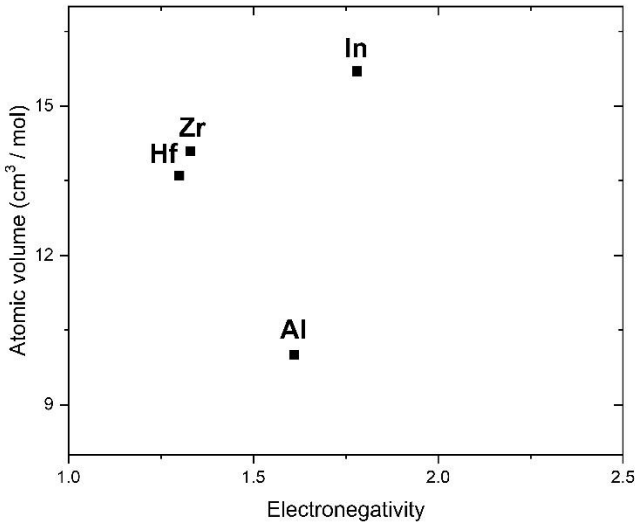

Figure 3: Comparison of atomic volumes and Pauling electronegativities of the probe and compound constituent atoms.

It is interesting to examine why are the errors for the calculated EFGs of the Cd probe atoms in Zr_2Al and ZrAl, so much larger than in $ZrAl_3$ and Zr_2Al_3. In order to see into this, we will discuss five possible contributions to the error bar on the predicted EFG, that are: a choice of the exchange-correlation functional, size of the basis set used for the calculation, distance between two impurities in the (super)cell, crystal-dependent c/a – induced uncertainty, and neglecting zero-point corrections [57]. We examined the effect on the EFG of various sampling meshes and found a spread of ± 0.04 x 10^{21} V/m^2 for ZrAl and ± 0.02 x 10^{21} V/m^2 for Zr_2Al. The choice of the exchange-correlation functional can give errors up to ± 0.1 x 10^{21} V/m^2 [57] and neglecting zero-point corrections usually gives a contribution of ± 0.1 x 10^{21} V/m^2 to the error for the calculated V_{zz} [58]. From all the above we can conclude that decisive contribution to the errors of the calculated EFGs comes from the different distance between two impurities atoms and the deviation of the calculated c/a ratio from the experimental one. If we compare the distance between two Cd atoms in the investigated supercells, we observe that it is larger in Zr_2Al_3 (> 10 Å) and $ZrAl_3$ (> 13 Å) than in Zr_2Al (~ 9.8 Å) and ZrAl (~ 8.5 Å). The calculated c/a ratio in ZrAl deviates for more than 1.5% from the experimental value, much more than in others investigated compounds.

4. Summary

In summary, using first principles calculations, we have investigated the hyperfine interactions and site preference of dopants in zirconium aluminides. The obtained results are consistent with the view that Cd substitutes exclusively for Al in $ZrAl_3$ and Zr_2Al_3. Our calculations showed that in Zr_2Al Cd probe atoms substitute for Zr, but the possibility of Cd atoms being also incorporated at Al lattice sites cannot be excluded. They indicate that Cd can probably substitute on both Zr and Al lattice sites in Zr_2Al. The difference between the calculated and measured EFGs for Cd probe

atoms is considerable in the systems with smaller distance between two impurities atoms and larger deviation of the calculated c/a ratio from the experimental one.

Acknowledgement

This study was financially supported by the Ministry of Education, Science and Technological Development of the Republic of Serbia through the Agreement with Vinča Institute of Nuclear Sciences.

Data availability

The raw/processed data required to reproduce these findings can be obtained from the authors upon reasonable request.

References

1. D.J. McPherson and M. Hansen, "The System Zr-Al", Trans. ASM, 46 (1954) 354–374.
2. J. Murray, A. Peruzzi, J. P. Abriata, "The Al-Zr (Aluminium-Zirconium) System", J. Phase Equilib. 13 (1992) 277-291.
3. Derek O. Northwood, The Development and Applications of Zirconium Alloys, Materials & Design, 6 (1985) 58-70.
4. R. Tewari, G. K. Dey, N. Prabhu, Microstructural studies on phase evolution sequence in rapidly solidified Zr_3Al based binary and ternary alloys, Mater. Sci. Eng. A 304-306 (2001) 548-554.
5. R. Tewari, G. K. Dey, S. Banerjee, N. Prabhu, Microstructural evolution in Zr_3Al-Based Alloys during Various Long-Time Annealing Treatments, Metall. Mater. Trans. A 37A (2006) 49-58.
6. J. H. Li, Y. Gao, S. Liu, L. Mao, F. C. Zhang, Q. Li, The effects of alloy composition and annealing time on microstructure and mechanical properties of Zr_3Al-based alloys, Mater. Res. Innovations 19 SUPPL 9 (2015) 55-58.

7. R. J. Kematick, H. F. Franzen, Thermodynamic Study of the Zirconium-Aluminum System, J. Solid State Chem. 54 (1984) 226-234.
8. H. Bo, D. D. Liu, L. B. Liu, L. J. Zhang, Y. Du, X. Xiong, Z. P. Jin, Computational study of atomic mobilities in Al-Zr solid solutions and the growth of $ZrAl_3$ intermetallic phase, CALPHAD: Computer Coupling of Phase Diagrams and Thermochemistry 40 (2013) 34-40.
9. P. Ravindran, R. Asokamani, Electronic structure, phase stability, equation of state, and pressure-dependent superconducting properties of Zr_3Al, Phys. Rev. B 50 (1994) 668-678.
10. Seung-Tae Ahn, Yong-Gyoo Kim, Jai-Young Lee, Formation of the amorphous phase in Zr_2Al by hydrogen absorption and the effects of titanium substitution on the amorphization behaviour, J. Alloys Comp. 186 (1992) 45-52.
11. Jai-Young Lee, Woo-Cheal Choi, Yong-Gyoo Kim, Jeong-Yong Lee, Transformation Characteristics of Hydrogen-Induced Amorphization of the Ordered Zr_3Al Phase, Acta metall. mater. 39 (1991) 1693-1701.
12. D. K. Tappin, I. M. Robertson, H. K. Birnbaum, On the Formation of a Periodic Surface Structure on Zr_3Al during Anodic Dissolution, Acta mater. 44 (1996) 735-746.
13. E. Ma, Amorphization and metastable polymorphs of ordered intermetallics Zr_3Al and Ni_3Al, J. Mater. Res. 9 (1994) 592-597.
14. D. K. Tappin, I. M. Robertson, H. K. Birnbaum, Enhancement of the electron-irradiation-induced amorphization of Zr_2Ni and Zr_3Al by hydrogen, Phys. Rev. B 51 (1995) 14854-14860.
15. W. J. Meng, P. R. Okamoto, L. J. Thompson, B. J. Kestel, L. E. Rehn, Hydrogeninduced crystal to glass transformation in Zr_3Al, Appl. Phys. Lett. 53 (1988) 1820-1822.

16. L. E. Rehn, P. R. Okamoto, J. Pearson, R. Bhadra, M. Grimsditch, Solid-State Amorphization of Zr_3Al: Evidence of an Elastic Instability and First-Order Phase Transformation, Phys. Rev. Lett. 59 (1987) 2987-2990.
17. D. Geist, S. Ii, K. Tsuchiya, H. P. Karnthaler, G. Stefanov, C. Rentenberger, Nanocrystalline Zr_3Al made through amorphization by repeated cold rolling and followed by crystallization, J.Alloys Comp. 509 (2011) 1815-1818.
18. M. Paljević, Z. Ban, Comparison of the oxidation behaviour of α-Zr-Al and Zr_3Al, J. Less Comm. Metals 95 (1983) 105-113.
19. M. Paljević, Z. Ban, Selective oxidation of zirconium in Zr_3Al, J. Less Comm. Metals 105 (1985) 83-86.
20. M. Paljević, Interaction of Zr_2Al with oxygen at high temperatures, J. Less Comm. Metals 120 (1986) 293-299.
21. P. B. Desch, R. B. Schwarz, P. Nash, Formation of metastable $L1_2$ phases in Al_3Zr and Al-12.5%X-25%Zr (X = Li, Cr, Fe, Ni, Cu), J. Less Comm. Metals 168 (1991) 69-80.
22. A. Laik, K. Bhanumurthy, G. B. Kale, Intermetallics in the Zr-Al diffusion zone, Intermetallics 12 (2004) 69-74.
23. D. Geist, C. Rentenberger, H. P. Karnthaler, High pressure torsion of intermetallic Zr_3Al, Mater. Sci. Forum 584-586 (2008) 553-558.
24. Atsushi Teruya, Masataka Takeda, Ai Nakamura, Hisatomo Harima, Yoshinori Haga, Kiyoharu Uchima, Masato Hedo, Takao Nakama, Yoshichika Ōnuki, Characteristic Fermi Surface Properties of V_2Ga_5, $CoGa_3$, $TiGa_3$, $ZrGa_3$, and $ZrAl_3$ with Different Tetragonal Structures, J. Phys. Soc. Japan 84 (2015) 054703.

25. Xiao-Li Yuan, Dong-Qing Wei, Xiang-Rong Chen, Qing-Ming Zhang, Zi-Zheng Gong, The first-principles calculations for the elastic properties of Zr_2Al under compression, J. Alloys Comp. 509 (2011) 769-774.
26. Jinliang Ning, Xinyu Zhang, Jiaqian Qin, Shiliang Zhang, Mingzhen Ma, Riping Liu, Distinct electron density topologies and elastic properties of two similar omega phases: ω-Zr and Zr_2Al, J. Alloys Comp. 660 (2016) 316-323.
27. Y. H. Duan, B. Huang, Y. Sun, M. J. Peng, S. G. Zhou, Stability, elastic properties and electronic structures of the stable Zr-Al intermetallic compounds: A first-principles investigation, J. Alloys Comp. 590 (2014) 50-60.
28. Leini Wang, Songjun Hou, Dewei Liang, First-principles investigations on the phase stability, elastic and thermodynamic properties of Zr-Al alloys, International J. Modern Phys. C 26, no 12 (2015) 1550143 (12 pages).
29. G. Ghosh, M. Asta, First-principles calculation of structural energetics of Al-TM (TM = Ti, Zr, Hf) intermetallics, Acta Mater. 53 (2005) 3225-3252.
30. G. Ghosh, A. van de Walle, M. Asta, First-principles calculations of the structural and thermodynamic properties of bcc, fcc and hcp solid solutions in the Al-TM (TM = Ti, Zr, and Hf) systems: A comparison of cluster expansion and supercell methods, Acta Mater. 56 (2008) 3202-3221.
31. P. S. Ghosh, A. Arya, R. Tewari, U. D. Kulkarni, G. K. Dey, Ab initio study on the formation of chemically ordered Zr_2Al phase by coupled replacive-displacive transformation, Philos. Mag. 92 no 33 (2012) 4040-4055.

32. Jefferson Z. Liu, G. Ghosh, A. van de Walle, M. Asta, Transferable force-constant modelling of vibrational thermodynamic properties in fcc-based Al-TM (TM = Ti, Zr, Hf) alloys, Phys. Rev. B 75 (2007) 104117.
33. Xiu Shang, Jiang Shen, Fuyang Tian, A first-principles study of the tetragonal and hexagonal R_2Al (R = Cr, Zr, Nb, Hf, Ta) phases, Mater. Res. Express 3 (2016) 106503.
34. Xiao-Li Yuan, Dong-Qing Wei, Yan Cheng, Guang-Fu Ji, Qing-Ming Zhang, Zi-Zheng Gong, Pressure effects on elastic and thermodynamic properties of Zr_3Al intermetallic compound, Comput. Mater. Sci. 58 (2012) 125-130.
35. Nihat Arikan, The first-principles study on Zr_3Al and Sc_3Al in $L1_2$ structure, J. Phys. Chem. Solids 74 (2013) 794-798.
36. D. Nguyen-Manh, D. G. Pettifor, Electronic structure, phase stability and elastic moduli of AB transition metal aluminides, Intermetallics 7 (1999) 1095-1106.
37. V. Koteski, H. -E. Mahnke, J. Belošević-Čavor, B. Cekić, G. Schumacher, Experimental and theoretical study of lattice relaxation around refractory atoms in nickel, Acta Mat. 56 (2008) 4601-4607.
38. A. Umićević, H. -E. Mahnke, J. Belošević-Čavor, B. Cekić, G. Schumacher, I. Mađarević, V. Koteski, Site preference and lattice relaxation around 4d and 5d refractory elements in Ni_3Al, Journal of Synchrotron Radiation 23 (2016) 286-292.
39. P. Wodniecki, B. Wodniecka, A. Kulinska, M. Uhrmacher, K. P. Lieb, The Zr_2Al and Zr_3Al compounds studied by PAC with ^{181}Ta and ^{111}Cd probes, J. Alloys Comp. 365 (2004) 52-57.

40. P. Wodniecki, B. Wodniecka, A. Kulinska, M. Uhrmacher, K. P. Lieb, Hf and Zr aluminides with B_f-type structure studied by PAC with ^{181}Ta and ^{111}Cd probes, J. Alloys Comp. 351 (2003) 1-6.
41. L. C. Damonte, L. A. Mendoza-Zelis, PAC Studies on Zr-Based Intermetallic Compounds, Hyp. Inter. 158 (2004) 317-322.
42. P. Wodniecki, B. Wodniecka, A. Kulinska, M. Uhrmacher, K. P. Lieb, The Electric Field Gradients in (Zr/Hf)Al_3 and (Zr/Hf)$_2Al_3$ Intermetallic Compounds Studied by ^{181}Ta- and ^{111}Cd-PAC Spectroscopy, Hyp. Inter. 136-137 (2001) 535-539.
43. P. Wodniecki, B. Wodniecka, A. Kulinska, M. Uhrmacher, K. P. Lieb, The $HfAl_2$ and $ZrAl_2$ Laves phases studied by ^{181}Ta and ^{111}Cd perturbed angular correlation spectroscopy, J. Alloys Comp. 335 (2002) 20-25.
44. P. Wodniecki, A. Kulinska, B. Wodniecka, M. Uhrmacher, K. P. Lieb, Solution of ^{111}In impurities in the Hf(Zr)$_3Al_2$ minority phases of Hf(Zr)$_4Al_3$ samples, Hyp. Int. 177 (2007) 11-117.
45. P. Wodniecki, A. Kulinska, B. Wodniecka, S. Cottenier, H. M. Petrilli, M. Uhrmacher, K. P. Lieb, Structural characterization of the Zr_4Al_3 and Hf_4Al_3 compounds by means of hyperfine interaction studies, Europhys. Lett. 77 (2007) 43001.
46. J. Belošević-Čavor, V. Koteski, B. Cekić, A. Umićević, Ab-initio calculation of electronic structure and electric field gradients in $HfAl_2$ and $ZrAl_2$ Laves phases, Comput. Mater. Sci. 41 (2007) 164-167.
47. L. A. Errico, H. M. Petrilli, L. A. Terrazos, A. Kulinska, P. Wodniecki, K. P. Lieb, M. Uhrmacher, J. Belošević-Čavor, V. Koteski, Electric field gradients in ^{111}In-doped

$(Hf/Zr)_3Al_2$ and $(Hf/Zr)_4Al_3$ mixed compounds: ab initio calculations, perturbed angular correlation measurements and site preference, J. Phys.:Condens. Matter 22 (2010) 215501.

48. P. Blaha, K. Schwarz, G. K. H. Madsen, D. Kvasnicka, J. Luitz, WIEN 2k an Augmented Plane Wave Plus Local Orbitals Program for Calculating Crystal Properties, Vienna University of Technology, Vienna, Austria, 2001.
49. J. P. Perdew, K. Burke, M. Ernzerhof, Generalized Gradient Approximation Made Simple, Phys. Rev. Lett. 77 (1996) 3865-3868.
50. P. E. Blochl, O. Jepsen, O. K. Andersen, Improved tetrahedron method for Brillouin-zone integrations, Phys. Rev. B 49 (1994) 16223-16233.
51. P. Blaha, K. Schwarz, P. Herzig, First-Principles Calculation of the Electric Field Gradient of Li_3N, Phys. Rev. Lett. 54 (1985) 1192-1195.
52. A. Kokalj, XCrysDen – A New Program for Displaying Crystalline Structures and Electron Densities, J. Mol. Graphics Modell. 17 (1999) 176-179.
53. P. Villars, L. D. Calvert, Pearson's Handbook of Crystallographic Data for Intermetallic Phases, ASM Materials Park, Ohio, 1996.
54. Y. Ma, C. Romming, B. Lebech, J. Gjonnes, A. Tafto, Acta Crystallogr. Sec. B 48 (1992) 11.
55. K. Lejaeghere, V. Van Speybroeck, G. Van Oost, S. Cottenier, Error Estimates for Solid-State Density-Functional Theory Predictions: An Overview by Means of the Ground-State Elemental Crystals, Critical Rev. Solid State Mater. Sci. 39 (2014) 1-24.
56. F. D. Murnaghan, Proc. Natl. Acad. Sci. U. S. A. **30**, 244 (1944).
57. Leonardo Errico, Kurt Lejaeghere, Jorge Runco, S. N. Mishra, Mario Renteria, Stefaan Cottenier, Precision of Electric-Field Gradient Predictions by Density Functional Theory

and Implications for the Nuclear Quadrupole Moment and Its Error Bar of the ^{111}Cd 245 keV $5/2^{+}$ Level, J. Phys. Chem. C 120 (2016) 23111-23120.

58. D.Torumba, K. Parlinski, M. Rots, S. Cottenier, Temperature Dependence of the Electric-Field Gradient in hcp-Cd from First Principles, Phys. Rev. B74 (2006) 144304.